11270 *Inorg. Chem.* **2010**, *49*, 11270–11275
DOI: 10.1021/ic101266d

Inorganic Chemistry
Article

Structure and Bonding of γ-B_{28}: Is the High Pressure Form of Elemental Boron Ionic?

Ulrich Häussermann*,† and Arkady S. Mikhaylushkin‡

†*Department of Chemistry and Biochemistry, Arizona State University, Tempe, Arizona 85287-1604, and*
‡*Department of Physics, Chemistry and Biology, Linköping University, SE 58133 Linköping, Sweden*

Received June 25, 2010

The recently characterized crystal structure of metastable γ-B_{28} is analyzed from a crystal chemical point of view, and the electron requirement of its building units and that of their linkage is determined. The structure consists of unique B_2 dumbbells and B_{12} icosahedra, which are connected through two-center and three-center, two-electron bonds. The different bonding motifs are ascertained by theoretical calculations of difference charge distributions. Chemical bonding in high pressure γ-B_{28} bears great resemblance to α-B_{12} which is the simplest boron modification. The previously made description of γ-B_{28} as ionic in terms of $(B_2)^{\delta+}$ and $(B_{12})^{\delta-}$ is not supported.

1. Introduction

Boron is a fascinating element with unique structures, bonding, and physical properties.[1] The central unit of its elemental structures and that of many boron rich compounds is a B_{12} icosahedron, which can be flexibly linked, joined, or fused into rigid framework structures. The occurrence of the B_{12} unit and its versatile connectivity is attributed to the "electron deficiency", or rather hypovalency, of boron. The understanding and rationalization of polyhedral boron structures represented a triumph of early quantum chemistry.[2] Today electron-counting rules for boron clusters and their linkages are well established and have even become text book knowledge.[3−5]

Still challenges remain. One example, obviously of rather fundamental nature, is the question of the actual ground state of boron. Previously it has been assumed that the simple and ordered α-modification (α-B_{12} with 12 atoms in the rhombohedral unit cell) is more stable than complex and disordered β-boron at zero temperature; the latter being considered as high temperature modification. Recent computations, however, point to the exciting possibility that β-boron is the most stable phase of boron down to temperatures very close to zero.[6,7] There β-boron corresponds to a geometrical frustrated system with macroscopic residual entropy because (high temperature) structural disorder leads to a multitude of energetically equivalent atomic configurations (at low temperature).[8]

Another example is the high pressure γ-modification of boron (γ-B_{28} with 28 atoms in the orthorhombic unit cell). Originally discovered in 1965,[9] γ-B_{28} has been recently resynthesized, and its structure and properties have been characterized.[10−12] It was found that γ-B_{28} is a superhard semiconductor with a structure composed of B_2 dumbbells and B_{12} icosahedra. Somewhat surprisingly it was concluded that bonding between these two distinct structural units should be partially ionic,[12] which attracted considerable attention.[13,14] The characterization of this well ordered boron modification invites for a closer analysis of its structure and bonding, and a critical examination of the issue "ionic elemental structures". We performed a comparative study

*To whom correspondence should be addressed. E-mail: ulrich.haussermann@asu.edu.

(1) Albert, B.; Hillebrecht, H. *Angew. Chem., Int. Ed.* **2009**, *48*, 8640, and references therein.
(2) Hoffmann, R.; Lipscomb, W. N. *J. Chem. Phys.* **1962**, *37*, 2872.
(3) (a) Wade, K. *J. Chem. Soc., Chem. Comm.* **1971**, 792. (b) Wade, K. *Inorg. Nucl. Chem. Lett.* **1972**, *8*, 559.
(4) (a) Jemmis, E. D.; Balakrishnarajan, M. M.; Pancharatna, P. D. *J. Am. Chem. Soc.* **2001**, *123*, 4313. (b) Jemmis, E. D.; Balakrishnarajan, M. M. *J. Am. Chem. Soc.* **2001**, *123*, 4324. (c) Prasad, D. L. V. K.; Balakrishnarajan, M. M.; Jemmis, E. D. *Phys. Rev. B* **2005**, *72*, 195102.
(5) (a) Burdett, J. K.; Canadell, E. *J. Am. Chem. Soc.* **1990**, *112*, 7207. (b) Burdett, J. K.; Canadell, E. *Inorg. Chem.* **1991**, *30*, 1991.
(6) Widom, M.; Mihalkovic, M. *Phys. Rev. B* **2008**, *77*, 064113.
(7) Ogitsu, T.; Gygi, F.; Reed, J.; Motome, Y.; Schwegler, E.; Galli, G. *J. Am. Chem. Soc.* **2009**, *131*, 1903.
(8) Ogitsu, T.; Gygi, F.; Reed, J.; Motome, Y.; Schwegler, E.; Galli, G. *Phys. Rev. B* **2010**, *81*, 020102(R).
(9) Wentorf, R. H. *Science* **1965**, *147*, 49.
(10) Zarechnaya, E. Y.; Dubrovinsky, L.; Dubrovinskaya, N.; Miyajima, N.; Filinchuk, Y.; Chernyshov, D.; Dimitriev, V. *Sci. Tech. Adv. Mater.* **2008**, *9*, 044209.
(11) Zarechnaya, E. Y.; Dubrovinsky, L.; Dubrovinskaya, N.; Filinchuk, Y.; Chernyshov, D.; Dimitriev, V.; Miyajima, N.; Goresy, A. E.; Braun, H. F.; van Smaalen, S.; Kantor, A.; Prakapenka, V.; Hanfland, M.; Mikhaylushkin, A. S.; Abrikosov, I. A.; Simak, S. I. *Phys. Rev. Lett.* **2009**, *102*, 185501.
(12) Oganov, A, R.; Chen, J.; Gatti, C.; Ma, Y.; Ma, Y.; Glass, C. W.; Liu, Z.; Yu, T.; Kurakevych, O. O.; Solozhenko, V. L. *Nature* **2009**, *460*, 292.
(13) Tse, J. S. *Nature* **2009**, *457*, 800.
(14) Withers, N. *Nat. Chem.* **2009**, *1*, 23.

 Published on Web 08/23/2010

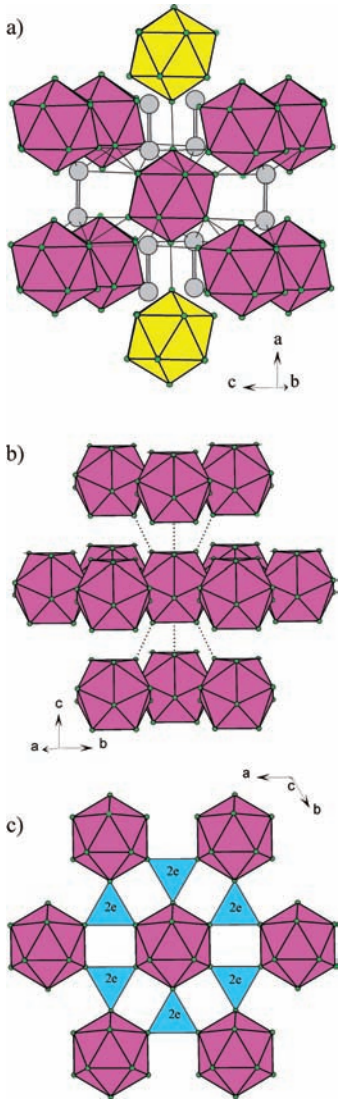

Figure 1. (a) Crystal structure of orthorhombic γ-B_{28} composed of icosahedral B_{12} units and B_2 dumbbells (gray). Each icosahedron is surrounded by 10 neighboring ones, two of which (yellow) are connected via terminal 2c2e bonds along the *a* direction. The remaining eight (purple) are joined via 3c2e bonds (cf. Figure 3). (b) Crystal structure of rhombohedral α-B_{12} corresponding to a cubic close packed arrangement of icosahedral B_{12} units (purple). Terminal 2e2c bonds connecting icosahedra between layers are indicated as broken lines. (c) Arrangement of B_{12} units within a close packed layer. Intralayer 3c2e bonds are indicated as blue triangles.

of α-B_{12} and γ-B_{28} with the aim of rationalizing the latter on the grounds of established electron-counting schemes and identifying the essential bonding features from computed difference charge densities.

2. Crystal Structure and Simple Bonding Analysis of γ-B_{28}: Similarities and Differences to α-B_{12}

The structure of γ-B_{28} is depicted in Figure 1a. The orthorhombic unit cell contains two B_2 dumbbells and two B_{12} icosahedra. Each icosahedron is surrounded by 10 neighboring ones, the distances between centers are 5.06 Å (2) and 5.16 Å (8), and six B_2 units.[11] In rhombohedral α-B_{12} (shown in Figure 1b,c) B_{12} icosahedra have 12 neighbors, that

(15) Will, G.; Kiefer, B. *Z. Anorg. Allg. Chem.* **2001**, *627*, 2100.

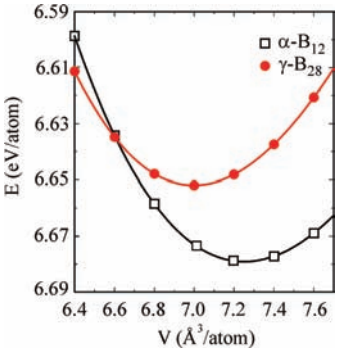

Figure 2. Computed total energy as a function of volume for α-B_{12} (black line, squares) and γ-B_{28} (red line, circles).

are arranged as in a cubic close packing at distances of 4.9 Å (6) and 5.08 Å (6).[15] The insertion of B_2 units between icosahedra makes γ-B_{28} about 3% denser than α-B_{12}. Figure 2 shows the calculated energy versus volume curves for both modifications. The equilibrium volume per atom is 7.0 and 7.22 Å^3 for γ-B_{28} and α-B_{12}, respectively (7.1 and 7.32 Å^3 experimentally). γ-B_{28} is by 0.028 eV/atom (2.9 kJ/mol) less stable than α-B_{12}.

The bonding situation in α-B_{12} is well understood by employing established electron-counting schemes.[16] According to Wade's rules,[3] skeleton bonding within an icosahedron B_{12} (36 electrons) requires 26 electrons, leaving 10 electrons for intercluster bonding. Terminal (exo) two-center, two-electron (2c2e) bonds (6 per cluster) connect icosahedra between close packed layers (broken lines in Figure 1b) while 3c2e bonds (also 6 per cluster) join them within layers (blue colored triangles in Figure 1c). For terminal (interlayer) bonding 6 electrons per cluster are used, while 3c2e (intralayer) bonding requires $2e/3 \times 6 = 4$ electrons. The different bonding motifs (skeleton, terminal 2c2e, and intralayer 3c2e) are well reflected in the distribution of involved B−B interatomic distances: those range from 1.75 to 1.81 Å for skeleton bonded atoms within clusters, and are 1.67 Å and 2.01 Å for 2c2e and 3c2e connected atoms, respectively (Table 1). These nearest neighbor distances associated with bonding interactions are well separated from the next nearest ones, starting off at 2.68 Å.

The situation for γ-B_{28} can be resolved on the same principles, although the distinctly different B−B distances occurring for the different bonding modes in α-B_{12} are blurred in γ-B_{28}. The range of nearest neighbor distances within B_{12} units (skeleton bonding) is larger than in α-B_{12} (1.74−1.88 Å), 2e2c and 3c2e bond lengths are between 1.61 and 1.72 Å, and 1.83 and 2.10 Å, respectively (Table 1). The clear separation of nearest neighbor distances from next nearest neighbor ones, starting off at 2.66 Å, however, is still present.

First, a closer look at the B_2 dumbbell and its environment by six B_{12} units is useful (Figure 3a). Two of the B_{12} units (yellow colored in Figure 3a) are connected to B_2 by short distances (1.61 Å) which can be associated with 2e2c bonds. Likewise corresponds the B−B distance within the dumbbell (1.66 Å) to a 2c2e bond. The shortest B−B distances between B_2 and the remaining four B_{12} units are 1.98 and 2.10 Å and, thus, relate to B−B distances associated with 3c2e bonding in

(16) Müller, U. *Inorganic Structural Chemistry*; John Wiley & Son: Chichester, 1993; p 104.

Table 1. Interatomic Distances (in Å and Organized According to Bonding Motifs), Coordination Numbers, and Bader Charges for Atoms in the α-B_{12} and γ-B_{28} Structures[a]

	skeleton bonds		2c2e bonds		3c2e bonds		CN	Q_{Bader}
			α-B_{12} ($R\bar{3}m$)					
B1 (18h)	−B1×2	1.754	−B1×1	1.671			1 + 5	+0.06
	−B2×1	1.800						
	−B2×2	1.807						
B2 (18h)	−B2×2	1.785			−B2×2	2.013	5 + 2	−0.06
	−B1×1	1.807						
	−B1×2	1.754						
			γ-B_{28} (*Pnnm*)					
B1 (4g)			−B4×1	1.606	−B2×2	1.983	2 + 4	+0.25
			−B1×1	1.659	−B3×2	2.101		
B2 (8h)	−B2×1	1.765			−B3×1	1.826	5 + 2	−0.17
	−B5×1	1.814			−B1×1	1.983		
	−B4×1	1.821						
	−B3×1	1.831						
	−B3×1	1.849						
B3 (8h)	−B5×1	1.758			−B2×1	1.826	5 + 2	0.00
	−B4×1	1.784			−B1×1	2.101		
	−B2×1	1.831						
	−B2×1	1.849						
	−B3×1	1.881						
B4 (4g)	−B5×1	1.737	−B1×1	1.61			1 + 5	+0.06
	−B3×2	1.784						
	−B2×2	1.821						
B5 (4g)	−B4×1	1.737	−B5×1	1.72			1 + 5	+0.03
	−B3×2	1.758						
	−B2×2	1.814						

[a]According to the parameters given in refs 11 and 15. The syntax of the coordination numbers reflects the bonding motifs.

α-B_{12}. 3c2e bonding in γ-B_{28} takes place between two B atoms of different icosahedra (purple colored in Figure 3a), 1.83 Å apart, and a B atom of the B_2 dumbbell. The resulting triangles are not equilateral as in α-B_{12}, and their arrangement is highlighted in Figure 3a. By so identifying 3c2e bonding in γ-B_{28}, each B atom of the B_2 dumbbell attains a quasi-tetrahedral environment by two 2c2e bonds and two triangles (Figure 3b), suggesting sp^3 hybridization. Two of the sp^3 orbitals and two electrons are involved in 2e2c bonding, the remaining two orbitals and one electron are used for 3c2e bonding (1 orbital and 0.5 electrons per triangle).

Next we turn to the coordination of the B_{12} units in γ-B_{28}. Each icosahedron is terminally bonded to two neighboring clusters (yellow colored in Figure 1a) and two B_2 units. The corresponding B−B distances are 1.72 and 1.61 Å, respectively. Additionally there are eight 3c2e bonds (triangles) to remaining icosahedra (8) and B_2 units (4). This is shown in Figure 3c. Again, skeleton bonding of the B_{12} unit (36 electrons) requires 26 electrons, which leaves 10 electrons for bonding to neighboring units. Four electrons are utilized in 2e2c terminal bonding, while 3c2e bonding requires $1.5e/2 \times 8 = 6$ electrons per icosahedron. (Reminder: a 3c2e bond in γ-B_{28} involves two B atoms of two icosahedra and one B atom of a B_2 unit; 0.5 electrons per bond are contributed from the latter.) The electron counts for the structural units in α-B_{12} and γ-B_{28} and their linkage are summarized in Table 2.

This analysis of the γ-B_{28} structure establishes firmly the electron requirement of its building units and their linkage. The presence of charged species $(B_2)^{\delta+}$ and $(B_{12})^{\delta-}$ as proposed in ref 12 is not supported. On the contrary, when assigning formal charges to the units from the electron-counting scheme by democratically dividing electrons for

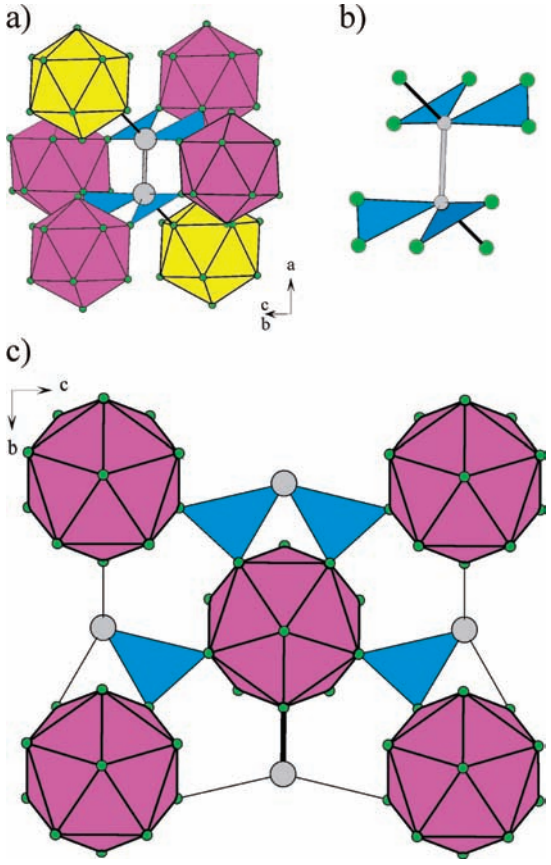

Figure 3. (a) Coordination environment of the B_2 dumbbell (gray) in γ-B_{28} in terms of B_{12} units. Yellow indicates 2e2c connected icosahedra, blue triangles indicate 3c2e bonds. (b) Coordination environment of the B_2 dumbbell in γ-B_{28} in terms of 2c2e bonds (thick black lines) and 3c2e bonds (blue triangles). (c) Arrangement of 3c2e bonds (blue triangles, 8 in total) and 2e2c bonds to a B_2 unit (thick black line, 2 in total) around a B_{12} unit in γ-B_{28}. Only the upper half along the *a* direction (four triangles and one 2c2e bond) is shown for clarity.

Table 2. Electron Counts (Italics) for Structural Units and Their Linkage in α-B_{12} and γ-B_{28}

	structure unit		linkage	
α-B_{12}	B_{12}		6 × 2c2e	6 × 3c2e
	26		*6 × 2/2*	*6 × 2/3*
γ-B_{28}	B_{12}		4 × 2c2e	8 × 3c2e
	26		*4 × 2/2*	*8 × 2/3*
	B_2		2 × 2c2e	4 × 3c2e
	2		*2 × 2/2*	*4 × 2/3*

linkage (B_{12}: 36e − 26e (skeleton) − 4e (2c2e) − 8 × 2/3e (3c2e) = +2/3; B_2: 6e − 2 (skeleton) − 2 (2c2e) − 4 × 2/3 (3c2e) = −2/3) a reverse situation is obtained. Chemically, the border case of B_{12}^{2-} units is only reasonable for all-exo bonded clusters (as, for example, in classic $B_{12}H_{12}^{2-}$), that is, when all cluster B atoms are terminated by 2c2e bonds and thus display a 1 + 5 coordination. As for α-B_{12}, this is not the case for γ-B_{28}. Likewise, B_2^{2+} would correspond to a (not viable) hypovalent species, where terminating ligands are expected to arrange linearly. While an ionic border case description $(B_2)^{2+}(B_{12})^{2-}$ for γ-B_{28} does not appear reasonable, some features of γ-B_{28} remain peculiar: (i) The coordination and bonding of the B_2 dumbbell atoms. Those atoms are involved in two 2c2e bonds, a bonding situation which has not been known for boron modifications. (ii) The triangle

defining the 3c2e bond in γ-B_{28} is rather unsymmetric in comparison with the equilateral triangle defining the corresponding bond in α-B_{12}. In the following we look at these features more closely by comparing and analyzing difference charge densities for α-B_{12} and γ-B_{28}.

3. Difference Charge Densities in α-B_{12} and γ-B_{28}

Analysis of charge density distributions is a classical way to extract bonding properties.[17] In this respect α-B_{12} has been the subject of several studies, both based on experimentally determined[15,18,19] and calculated charge densities.[20,21] However, findings were not always consistent. The charge density of γ-B_{28} has only been fragmentarily analyzed in refs 11 and 12. To obtain difference charge densities, $\Delta\rho$, the charge of a superposition of non-interacting atoms is subtracted. This typically enhances the features related with bonding properties.

Figure 4 displays the results for α-B_{12}. The two different kinds of boron atoms are distinguished as polar (p) and equatorial (e).[18] Polar atoms carry terminal 2c2e bonds, equatorial ones perform 3c2e bonding between B_{12} clusters (eee triangles). Three different kinds of icosahedral triangles, ppp, ppe, and pee mirror skeleton bonding (Figure 4a). Among the icosahedral triangles, ppp ones are distinguished because they are equilateral and display the shortest distances. They also display the highest $\Delta\rho$ values, with a maximum at the center (for symmetry reasons). The $\Delta\rho$ distribution in the ppe and pee triangles is notably different (see Figure 4b). In pee triangles the maximum becomes located at the ee edge.[22] The $\Delta\rho$ distribution associated to 3c2e bonding (triangles eee) is the same as for ppp (for symmetry reasons); however, values are substantially lower.

Charge accumulation associated with 2c2e bonding is clearly enhanced compared to skeleton and 3c2e bonding. The balloon-shaped $\Delta\rho$ isosurfaces shown in Figure 4b correspond to a value of 0.22 e/Å^3. They actually enclose two local maxima which are located on opposite sites of the B−B interatomic line. This "bend bond" feature has been observed earlier in experimental charge density studies and has been attributed to the deviation of the rhombohedral angle of the α-B_{12} cell ($\sim$ 58°) from the angle between 5-fold axes of a regular icosahedron (63.43°).[18,19] We note that the bonding features for α-B_{12} extracted from our calculated $\Delta\rho$ distribution are in large agreement with the recent analysis of an experimental charge density distribution performed by Hosoi et al.[19]

With α-B_{12} as a reference we now turn to γ-B_{28} (Figure 5). First, $\Delta\rho$ values are generally higher because of the higher density of the high pressure phase. Second, the icosahedra are much less symmetric and are composed of 6 different triangles. Accordingly, the $\Delta\rho$ distribution in these triangles, expressing skeleton bonding, varies substantially (Figure 5a, 5c). Highest values of $\Delta\rho$, along with a maximum close to the center, are found in triangles B3B4B5 which have the shortest edges (1.74−1.78 Å). In contrast, in triangles B2B3B3 with the longest edges (1.85−1.88 Å) $\Delta\rho$ values are comparably low.

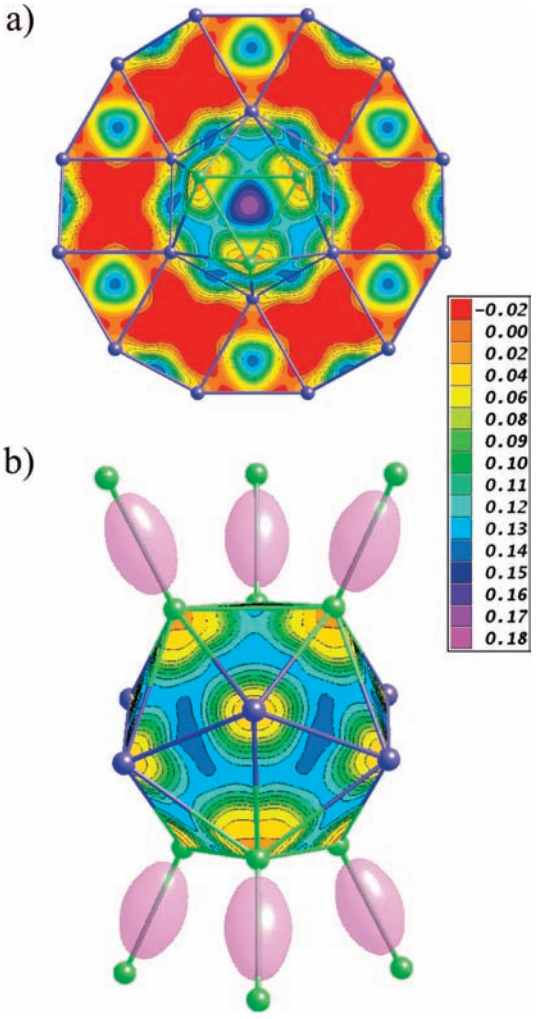

Figure 4. Difference charge density distribution in α-B_{12}. Contour maps are shown for planes expressing skeleton and 3c2e bonding. The levels are indicated by different colors. 2c2e bonds are represented as pink isosurfaces (value 0.22 e/Å^3). (a) Icosahedron and 3e2c bonds viewed along [001] with respect to the hexagonal unit cell of a-B12. (b) Icosahedron and 2e2c bonds viewed along [1$\bar{1}$0]. Polar (B1) and equatorial (B2) atoms are drawn as green and blue spheres, respectively.

The triangles B1B2B3 that were identified as 3c2e bonds in the previous section are indeed distinguished. Compared to other triangles between icosahedra (e.g., B1B2B2) they display substantial charge accumulation. As a matter of fact, this accumulation is larger than that associated with skeleton bonding. The $\Delta\rho$ maximum in B1B2B3, however, is pronouncedly shifted toward the short edge B2B3 (1.83 Å). Also the postulated 2c2e bonds from the electron-counting analysis are clearly identified (Figure 5b, 5c). The balloon-shaped $\Delta\rho$ isosurfaces shown in Figures 5b and 5c correspond to a value of 0.29 e/Å^3. Interestingly they all enclose two local maxima similar to the "bend" 2e2c bond in α-B_{12}. Note, that all 2e2c bonds in γ-B_{28} are situated on (002) planes. This plane has been analyzed in ref 11. The contacts B1B4, B1B1 and B5B5 were identified as strongly covalent.

In conclusion, our $\Delta\rho$ analysis for γ-B_{28} supports the electron-counting scheme established in the previous section.

(17) Koritsanszky, T. S.; Coppens, P. *Chem. Rev.* **2001**, *101*, 1583.
(18) Fujimoro, M.; Nakata, T.; Nakayama, T.; Nishibori, E.; Kimurea, K.; Takata, M.; Sadata, M. *Phys. Rev. Lett.* **1999**, *82*, 4452.
(19) Hosoi, S.; Kim, H.; Nagata, T.; Kirihara, K.; Soga, K.; Kimura, K.; Kato, K.; Takata, M. *J. Phys. Soc. Jpn.* **2007**, *76*, 0446602.
(20) Lee, S.; Bylander, D. M.; Kleinman, L. *Phys. Rev. B* **1990**, *42*, 1316.
(21) He, J.; Wu, E.; Wang, H.; Liu, R.; Tian, Y. *Phys. Rev. Lett.* **2005**, *94*, 015504.
(22) Here, the actual maximum of the three-dimensional $\Delta\rho$ distribution is slightly off the triangular plane. This is also observed for some triangular planes in less symmetric γ-B_{28}.

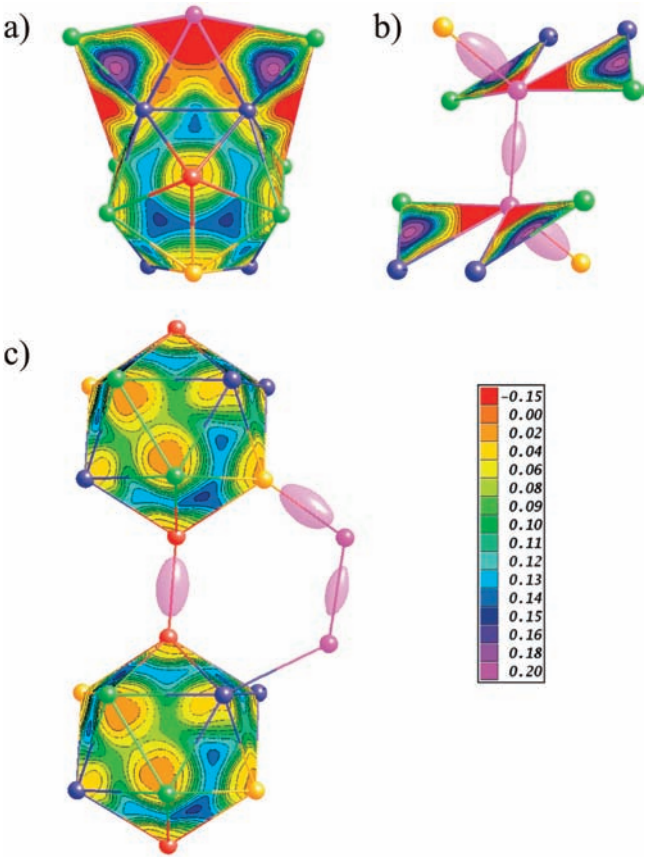

Figure 5. Difference charge density distribution in γ-B_{28}. Contour maps are shown for planes expressing skeleton and 3c2e bonding. The levels are indicated by different colors. 2c2e bonds are represented as pink isosurfaces (value 0.29 e/Å^3). (a) Icosahedron and 3e2c bonds viewed along [001], (b) Dumbbell B_2 unit with 2c2e and 3e2c bonds, (c) Two icosahedra and 2e2c bonds viewed approximately along [0$\bar{1}$1]. Dumbbell (B1) atoms are drawn as pink spheres. B2, B3, B4, and B5 atoms in icosahedra are drawn as blue, green, yellow, and orange spheres, respectively.

As for α-B_{12}, bonding in γ-B_{28} can be divided into skeleton, 2c2e, and 3c2e motifs. However, some features are notably different: (i) The $\Delta\rho$ distribution connected to skeleton bonding is rather irregular compared to α-B_{12} because of the lower symmetry of the icosahedra. (ii) The 3c2e bond is highly unsymmetrical and associated with a much high charge accumulation compared to α-B_{12}. Consequently, it may be speculated that the 3c2e bond in γ-B_{28} is considerably stronger. Finally, we return to the question of ionicity. The $\Delta\rho$ distributions shown in Figures 5a, 5b indicate indeed a greater charge depletion around the dumbbell B1 atoms than around the icosahedron forming ones.

4. Ionicity of Elemental Structures

A main reason for the ionicity of γ-B_{28} put forward in ref 12 was that Bader charges[23] obtained from the calculated electron density were found to be substantial, that is, +0.24 per B atom in a dumbbell. The assumption of an "ionic elemental structure" requires the presence of different crystallographic positions producing distinctively different coordination and/or bonding environments for atoms of the same element. In this respect also the structure of α-B_{12} is composed of two sites, that is, B atoms connected via 2c2e and 3c2e bonds, respectively, to neighboring icosahedra. However, in contrast to γ-B_{28} possessing two distinct structural units, the coordination environment of the two different B atoms in α-B_{12} is similar, and calculated Bader charges are just $\pm$0.057.[12]

It is not clear if and how calculated Bader charges account for ionicity in elemental structures. Out of curiosity we looked at the complex structure of α-Mn. It is composed of four different kinds of Mn atoms, which occur with multiplicities of 2, 8, 24, and 24.[24] Here the minority Mn atoms attain considerable positive charges, +0.21 and +0.19, which approach the situation found for the B_2 dumbbell atoms in γ-B_{28}.[25] Will this make α-Mn ionic? An important feature of the α-Mn structure is the simultaneous occurrence of low and high multiplicity sites, which allows that a rather large charge on the low multiplicity site (for whatever reason it occurs) is counterbalanced by small opposite charges on the majority component. The situation appears different for γ-B_{28} where the charges on the dumbbell atoms are largely balanced by just one type of B atoms (B2) within the icosahedra.

We recalculated the Bader charges of B atoms in γ-B_{28} and α-B_{12} and could confirm the finding of ref 12 (Table 1). Noticeably, positive charges always become associated with boron atoms that are involved in 2e2c bonds. It is highest for the dumbbell atoms forming two of such bonds. The 1 + 5 coordinated atoms being part of icosahedra attain similar and small positive charges in both structures. The 5 + 2 coordinated atoms with no terminal bond are neutral or negatively charged. B2 atoms in the γ-B_{28} structure are distinguished by their large charge of $-$0.17.

We are inclined to postulate that those Bader charges do not affect our established overall bonding picture for γ-B_{28}, other than adding some degree of bond polarity. The occurrence of bond polarity has also been discussed for α-B_{12}.[21] Especially, the Bader charges of B atoms in γ-B_{28} express by no means a (pressure-induced) extreme bonding situation for boron. This has now also been recognized by the authors of ref 12 who recently relativized their original, ionic, interpretation of γ-B_{28}.[26] As a matter of fact, when comparing the structures of α-B_{12} and γ-B_{28} it is easily understandable how the latter is adapted to high pressure. Generally, in both modifications boron atoms are either 6- or 7-coordinated (cf. Table 1). 7-coordinated atoms are part of icosahedra and involved in 3c2e linkage. As expected, the more dense high pressure form has a larger fraction of 7-coordinated atoms. In particular for α-B_{12}, half of the atoms forming icosahedra are 7-coordinated while for γ-B_{28} this fraction is 2/3. A larger fraction of 7-coordinated atoms implies a redistribution of the bonding motifs for linkage: The number of "electron efficient" 3c2e links is increased at the expense of "electron extensive" terminal (2c2e) ones (cf. Table 2). As a consequence, with respect to the linkage of B_{12} building units, electrons become "untied" in γ-B_{28}, and the significance of its peculiar B_2 dumbbell unit is to act as a "reservoir" for them.

(23) Bader, R. F. W. *Atoms in Molecules: A Quantum Theory*; Oxford University Press: Oxford, 1990.

(24) Oberteuffer, J. A.; Ibers, J. A. *Acta Crystallogr., Sect. B* **1970**, *26*, 1499.

(25) A similar result has been extracted from Mulliken population analyses of model systems with the α-Mn structure (Fredrickson, D. C.; Lee, S.; Hoffmann, R. *Angew. Chem.; Int. Ed.* **2007**, *46*, 1958).

(26) Oganov, A, R.; Chen, J.; Gatti, C.; Ma, Y.; Ma, Y.; Glass, C. W.; Liu, Z.; Yu, T.; Kurakevych, O. O.; Solozhenko, V. L. *Nature* **2009**, No. 457, 863.

5. Conclusions

Boron displays a uniquely flexible structural chemistry based on icosahedral units. In this respect, the recently characterized structure of its high pressure form γ-B_{28} added a new feature through the occurrence of B_2 dumbbells acting as novel linkers between icosahedral units. Analysis of structure and bonding of γ-B_{28} reveals surprising similarities to α-B_{12} which is the simplest boron modification. In both structures icosahedron forming atoms are involved in 2c2e and 3c2e bonding for linkage, being 6- and 7-coordinated, respectively. However, γ-B_{28} possesses a higher fraction of 7-coordinated atoms, and through the higher fraction of 3c2e links the electron count for linkage bonding is decreased. The unique B_2 dumbbell balances the altered electron count. The result of an earlier analysis describing γ-B_{28} as ionic in terms of $(B_2)^{\delta+}$ and $(B_{12})^{\delta-}$ is not supported.

6. Methods

Theoretical calculations of the electronic structure and total energies of α-B_{12}, γ-B_{28}, and α-Mn were performed by means of the first principles all-electron projector augmented waves (PAW) method[27] as implemented in the Vienna Ab Initio Simulation Package (VASP).[28] Exchange-correlation effects were treated within the generalized gradient approximations (GGA) using the Perdew−Burke−Ernzerhof (PBE) parametrization.[29] The structures were relaxed with respect to volume, lattice parameters, and atom positions. Forces were converged to better than 1×10^{-3} eV/Å. The integration over the Brillouin zone (BZ) was done on a grid of special k-points determined according to the Monkhorst−Pack scheme[30] and using the linear tetrahedron method with Blöchl correction.[31]

To achieve a very high accuracy charge density we increased substantially the cutoff energies, k-point grids, and grids for the fast Fourier transformation (FFT) with respect to the values necessary for the total-energy convergence. The cutoff energy was set to 600 eV and k-point grids of $12 \times 12 \times 12$ (γ-B_{28} and α-Mn) and $16 \times 16 \times 16$ (α-B_{12}) were employed. The mesh of the FFT grid was $360 \times 360 \times 360$. Bader analysis of charge densities was performed according to ref 32. The error of the calculated Bader charges is smaller than 0.01 e/atom. For obtaining difference charge densities, the charge density obtained for a superposition of atomic wave functions was subtracted from the charge density obtained for a self-consistent energy optimization.

Acknowledgment. This research has been supported by the ACS Petroleum Research Fund under the Grant 45796-AC10. A.S.M. acknowledges financial support from Linköping Linnaeus Initiative for Novel Functional Materials. For most calculations the computational resources of the Swedish National Infrastructure for Computing (SNIC) were used.

(27) (a) Blöchl, P. E. *Phys. Rev. B* **1994**, *50*, 17953. (b) Kresse, G.; Joubert, J. *Phys. Rev. B* **1999**, *59*, 1758.
(28) (a) Kresse, G.; Hafner, J. *Phys. Rev. B* **1993**, *48*, 13115. (b) Kresse, G.; Furthmüller, J. *Comput. Mater. Sci.* **1996**, *6*, 15.
(29) (a) Wang, Y.; Perdew, J. P. *Phys. Rev. B* **1991**, *44*, 13298. (b) Perdew, J. P.; Chevary, J. A.; Vosko, S. H.; Jackson, K. A.; Pederson, M. R.; Singh, D. J.; Fiolhais, C. *Phys. Rev. B* **1992**, *46*, 6671.
(30) Monkhorst, H. J.; Pack, J. D. *Phys. Rev. B* **1976**, *13*, 5188.
(31) Blöchl, P. E.; Jepsen, O.; Andersen, O. K. *Phys. Rev. B* **1994**, *49*, 16223.
(32) (a) Armaldsen, A.; Tang, W.; Henkelman, G. http://theory.cm.utexas.edu/bader/. (b) Tang, W.; Sanville, E.; Henkelman, G. *J. Phys.: Condens. Matter* **2009**, *21*, 084204.